



Short communication

## Co-MOF/titanium nanosheet array: An excellent electrocatalyst for non-enzymatic detection of H<sub>2</sub>O<sub>2</sub> released from living cells

Lian Xia<sup>a</sup>, Xiaoqian Luan<sup>a</sup>, Fengli Qu<sup>a,\*</sup>, Limin Lu<sup>b,\*</sup><sup>a</sup> College of Chemistry and Chemical Engineering, Qufu Normal University, Qufu 273165, Shandong, China<sup>b</sup> Institute of Functional Materials and Agricultural Applied Chemistry, College of Science, Jiangxi Agricultural University, Nanchang 330045, PR China

## ARTICLE INFO

## Article history:

Received 21 May 2020

Received in revised form 30 July 2020

Accepted 31 July 2020

Available online 5 August 2020

## Keywords:

Metal organic frameworks

Transition metal

Electrocatalyst

Hydrogen peroxide

Living cells

## ABSTRACT

In this study, a composite nanosheet array (Co-MOF/TM) was developed by in-situ growing the cobalt-based metal-organic framework (Co-MOF) on titanium mesh (TM) to fabricate a non-enzymatic electrochemical sensor for detection of H<sub>2</sub>O<sub>2</sub> released from living cells. The amperometric current in cyclic voltammetry (CV) enhanced linearly with the increase of H<sub>2</sub>O<sub>2</sub> concentration. Due to the unique properties of Co-MOF, the proposed sensor showed excellent H<sub>2</sub>O<sub>2</sub> detection performance, including low detection limits (0.25 μM, S/N = 3), wide linear range (1–13,000 μM, R > 0.995), high sensitivity (98.75 μA mM<sup>-1</sup> cm<sup>-2</sup>), fast response within 3 s, and high selectivity in PBS solution. More importantly, the proposed electrode can be used to in situ sensing H<sub>2</sub>O<sub>2</sub> released from A549 cells. This work provides a new design strategy of nonenzymatic electrochemical sensing method for amperometric determination of H<sub>2</sub>O<sub>2</sub> in biological environment and also shows high perspective for sensing other biomolecules using other active MOFs as electrocatalytic electrodes.

## 1. Introduction

Hydrogen peroxide (H<sub>2</sub>O<sub>2</sub>) plays an important role in physiological process, its concentration is recognized as an essential physiological parameter [1]. Abnormal concentration level of H<sub>2</sub>O<sub>2</sub> in living cells can cause the accumulation of oxidative stress, which can further lead to various diseases including cancer, diabetes, neurodegenerative, Alzheimer's, Parkinson's and Huntington's diseases [2–5]. Therefore, the monitoring of H<sub>2</sub>O<sub>2</sub> released from living cells is of significance for both physiological and pathological investigations [6,7]. Up to now, a number of analytical techniques have been reported for H<sub>2</sub>O<sub>2</sub> detection, such as fluorescence, colorimetry, high-performance liquid chromatography (HPLC), titrimetry, chemiluminescence, cell imaging and electrochemistry sensors [8–14]. In comparison with other methods for H<sub>2</sub>O<sub>2</sub> detection, electrochemical techniques show attractive attention due to their good sensitivity and selectivity, easy operating, fast response and cost-effective instrumentation [15].

Although high sensitivity and desirable selectivity have been achieved with enzymatic detection of H<sub>2</sub>O<sub>2</sub> based on electrocatalytic sensors, their inherent drawbacks, such as intrusive chemical and thermal instability of the enzyme, severely hinder their practical applications [16]. Therefore, non-enzymatic electrocatalytic sensors have been gained attractive attention in biological detection due to their characteristics of high stability and reliability, as well as good lifetime of modified electrodes [17,18]. To date, numerous non-enzymatic electrocatalytic sensors based on various

materials have been reported for the sensing of H<sub>2</sub>O<sub>2</sub> with satisfactory results, such as noble metals, transition metals, carbon materials. However, there are still some problems existed on these sensors, including high cost, easily poisoned by the adsorbed intermediates, and so on [19,20]. Therefore, it is significant and attractive to establish non-enzymatic electrochemical sensors with properties of high sensitivity, desirable selectivity, good reliability, low cost and electrode poisoning resistance for detection of H<sub>2</sub>O<sub>2</sub>.

Being one kind of new functional materials, metal-organic frameworks (MOFs) formed by joining metal ions with organic links through coordinate-covalent bond, have received great attentions for wide use in gas, luminescence, sensors and catalysis, due to their unique structural properties such as porous structure and high specific surface area [21,22]. Furthermore, many literatures reported that the MOFs formed by Co<sup>2+</sup> as the metal ion showed obvious catalysis activity [23–25]. Inspired by these characteristics of Co-MOFs, we envisaged that the electrode modified with Co-based MOFs can act as electrocatalysts for non-enzymatic detection of H<sub>2</sub>O<sub>2</sub>. Firstly, rich unsaturated metal sites of Co<sup>2+</sup> can provide catalytic active centers [26]. Secondly, the uniform porous structure of the MOFs has size-selective effect [27], which will prevent interference molecules and cells from adsorbing into the pores of the MOFs, thereby minimize the electrode poisoning. Thirdly, owing to the large surface area of the MOFs, the target molecules of H<sub>2</sub>O<sub>2</sub> can be absorbed on their numerous unsaturated metal sites, facilitating the catalytic reaction [28].

\* Corresponding authors.

E-mail addresses: [fengliqun@hotmail.com](mailto:fengliqun@hotmail.com), (F. Qu), [lulimin816@hotmail.com](mailto:lulimin816@hotmail.com). (L. Lu).

Herein, we designed a Co-MOF nanosheet array supported on Ti mesh (Co-MOF/TM) as a modified electrode for detection of H<sub>2</sub>O<sub>2</sub> released from living cells. The Co-MOF was synthesized by coordination of Co<sup>2+</sup> with terephthalic acid, which showed properties of good stability, high porosity, large surface area, and rich unsaturated Co<sup>2+</sup> sites. With the support of the Ti mesh, the nanosheet-structural Co-MOF enhanced its electrical conductivity and catalytic activity owing to the surface electronic defects. Therefore, the constructed electrode in this study possesses good electrical conductivity than previously reported MOFs and shows good electrochemical performance due to the fast electron transfer as well as the sensitive response to the target. Furthermore, the detection of the trace amount of H<sub>2</sub>O<sub>2</sub> secreted from living cells was successfully performed with this biosensor.

## 2. Experimental

### 2.1. Materials and reagents

CoCl<sub>2</sub>·6H<sub>2</sub>O was supplied by Xiya Reagent Co., Ltd. terephthalic acid (TPA), sodium dihydrogen phosphate (NaH<sub>2</sub>PO<sub>4</sub>), disodium hydrogen phosphate (Na<sub>2</sub>HPO<sub>4</sub>), ascorbic acid (AA), dopamine (DA), uric acid (UA), were supplied by Sigma-Aldrich (Shanghai, China), and *N,N*-Dimethyl formamide (DMF) was supplied by Sinopharm Chemical Reagent Beijing Co., Ltd. The ultrapure water used throughout all experiments through a Millipore system. All reagents were analytical reagent grade and used as received without further purification.

### 2.2. Preparation of Co-MOFs nanosheets array

The Co-MOF/TM was prepared by one-step solvothermal method according to the reported literature [29]. Briefly, CoCl<sub>2</sub>·6H<sub>2</sub>O (0.238 g) and TPA (0.166 g) were dissolved into 35 mL DMF with vigorous stirring for 10 min. Next, 2.5 mL ethanol and 2.5 mL ultrapure water were slowly added separately and stirred for 30 min. After that, the above solution was transferred into a 50 mL Teflon-lined stainless-steel autoclave with a piece of Ti mesh (2 × 4 cm), keeping 125 °C for 12 h. After cooling to room temperature naturally, collected the product and washed it with ultrapure water for three times. With drying at 60 °C for 4 h, the Co-MOF/TM was obtained.

### 2.3. Characterizations

X-ray diffraction (XRD) patterns were recorded with the Panalytical X-ray Diffractometer Model X pert3 employing Cu Kα radiation (λ = 1.5406 Å). Scanning electron microscope (SEM) measurements were recorded on a XL30 ESEM FEG scanning electron microscope at an accelerating voltage of 20 kV. X-ray photoelectron spectroscopy (XPS) data was collected on a Thermo ESCALAB 250XI x-ray photoelectron spectrometer using Mg as the exciting source.

### 2.4. Electrochemical measurements

Electrochemical experiments measurements were carried out on an electrochemical workstation (CHI 660E) with a standard three electrode system. The supporting electrolyte is 0.1 M PBS (pH = 7.4). Co-MOF/TM, graphite electrode and Ag/AgCl electrode were employed as working electrode, counter electrode and reference electrode, respectively. Note that all experimental data were carried out at room temperature.

## 3. Results and discussion

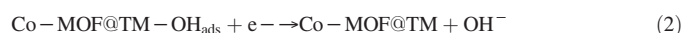
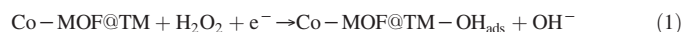
### 3.1. Characterization of the co-MOF/TM

The synthesized Co-MOF was firstly confirmed by XRD. As shown in Fig. 1a, the XRD patterns of the synthesized Co-MOF/TM in this study show good consistency with that of the simulated one, which indicated

that the Co-MOF was successfully composited with TM, and the crystalline of it remains well after composition. Fig. 1b shows the SEM image of Co-MOF/TM, the tightly packed nanosheets stacked together and grown on the bare TM. The energy-dispersive X-ray (EDS) elemental mapping analysis of Co-MOF/TM confirms the existence of Co, C and O elements in the product and those elements distribute in the whole nanoarray uniformly. The X-ray photoelectron spectroscopy (XPS) survey spectrum of Co-MOF/TM can further confirm the existence of Co, C and O elements (Fig. 1c). As revealed in Fig. 1d, the binding energies (BEs) at 797.5 and 781 eV can be indexed to Co 2p<sub>1/2</sub> and Co 2p<sub>3/2</sub> regions, respectively [30]. The peak at 786.8 and 804.1 eV are well fitted with two shakeup satellites (identified as "Sat.") [31]. These evidences can certify that the existence of Co<sup>2+</sup>.

### 3.2. Electrochemical performance of co-MOF/TM nanosheets

To identify the properties of electrochemical biosensor, we measured the performance of Co-MOF/TM electrode with typical three-electrode setup for detecting H<sub>2</sub>O<sub>2</sub>. As shown in Fig. 2a, the cyclic voltammeters (CVs) of TM and Co-MOF/TM were investigated in 0.1 M PBS (pH = 7.4), which measured in the absence and presence of 3 mM H<sub>2</sub>O<sub>2</sub> at a scan rate of 50 mV s<sup>-1</sup>. Bare TM (curves 1 and 2) shows a nearly similar current density in the absence and presence of H<sub>2</sub>O<sub>2</sub>, indicating that this electrode is electrochemically inert for the detection of H<sub>2</sub>O<sub>2</sub>. By contrast, the reduction current density of the Co-MOF/TM electrode (curves 3 and 4) presents notably increased after adding H<sub>2</sub>O<sub>2</sub>, indicating that the obtained Co-MOF/TM electrode is promising for H<sub>2</sub>O<sub>2</sub> detection. Fig. 2b shows the CVs responses of the Co-MOF/TM under different H<sub>2</sub>O<sub>2</sub> concentration from 1 to 7 mM. The cathode-current densities enhanced with the increasing H<sub>2</sub>O<sub>2</sub> concentration, which further indicated the sensing ability of Co-MOF/TM towards H<sub>2</sub>O<sub>2</sub>. In order to research the electrode kinetics, the effect of scan rate on the CVs response was investigated. As plotted in Fig. 2c, the response current of reduction peak rose with the increasing of scan rate in the range of 30 to 200 mV s<sup>-1</sup>. The electrocatalytic mechanism can be depicted as follows according to the reports [32]:



The amperometric responses of Co-MOF/TM to H<sub>2</sub>O<sub>2</sub> at various applied potentials were investigated to determine the optimum working potential. As shown in Fig. S1, the amperometric response of Co-MOF/TM enhanced significantly with the increasing of the absolute value of the applied potential in the presence of 1 mM H<sub>2</sub>O<sub>2</sub>. As we all know, the higher applied potential was employed, the severer interference will be suffered. And there was a satisfactory amperometric response when the applied potential was -0.4 V. Therefore, -0.4 V was selected as the optimum working potential in this study.

Once the working potential was selected, the sensing performance of the Co-MOF-TM to H<sub>2</sub>O<sub>2</sub> was to be investigated. Fig. 3a exhibits the amperometric response curve of the Co-MOF/TM electrode to H<sub>2</sub>O<sub>2</sub> concentrations, which changed with consecutive step from 0 μM to 1.3 mM in 0.1 M PBS at an applied potential of -0.4 V. It can be seen from Fig. 3a, the current shows apparently stepwise increase with successive addition of H<sub>2</sub>O<sub>2</sub>. As being plotted in Fig. 3b, the calibration curve of the current response vs H<sub>2</sub>O<sub>2</sub> concentration is in the range of 1 μM to 1.3 mM. There are two linear calibration plots corresponding to the low (1–310 μM) and medium (0.31–1.3 mM) concentration ranges. The two linear calibration plots are in good fit with the regression equations. Furthermore, the limit of detection was estimated to be 0.25 μM (S/N = 3), suggesting that the proposed Co-MOF/TM biosensor possesses superior electrochemical detection ability. The stability of the Co-MOF/TM biosensor is evaluated by recording successive CV responses of 1.0 mM H<sub>2</sub>O<sub>2</sub> 20 times. The results

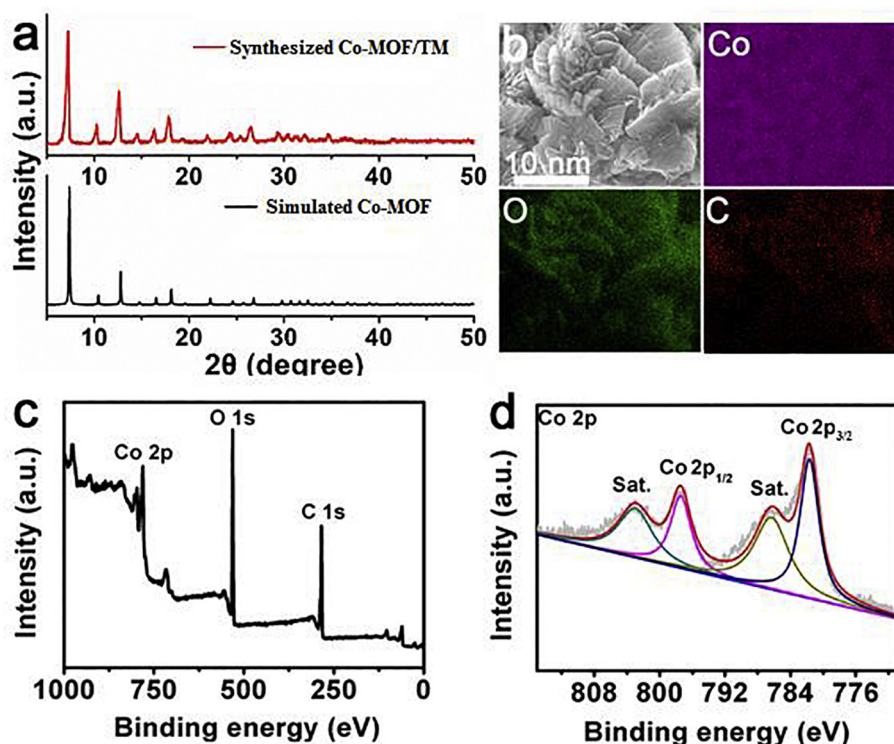


Fig. 1. (a) XRD pattern of the simulated Co-MOF and the synthesized Co-MOF/TM; (b) SEM image and EDS elemental mapping of Co-MOF/TM. (c) XPS survey spectrum for Co-MOF/TM. (d) XPS spectra of Co-MOF/TM in the Co 2p region.

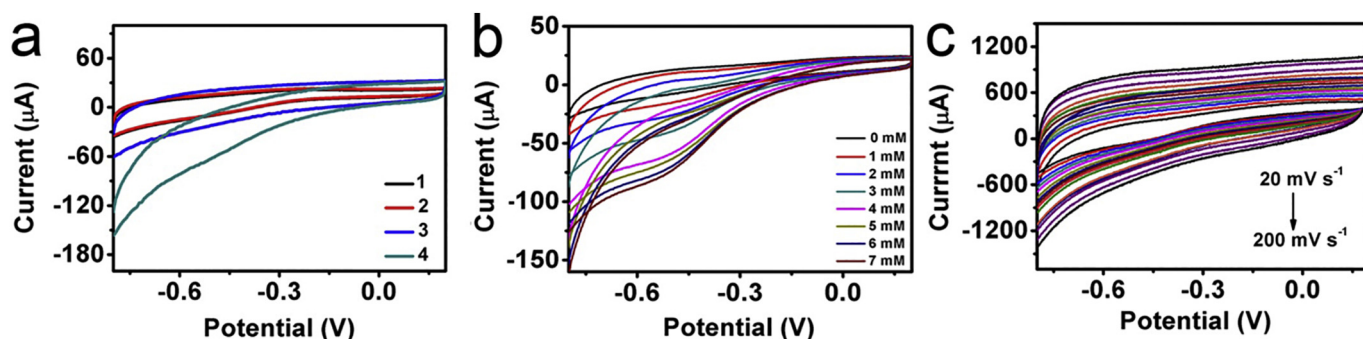


Fig. 2. (a) CVs of bare TM (curves 1 and 2) and Co-MOF/TM (curves 3 and 4) in the absence and presence of 3 mM  $\text{H}_2\text{O}_2$  in 0.1 M PBS (scan rate:  $50 \text{ mV s}^{-1}$ ) at a scan rate of  $50 \text{ mV s}^{-1}$ . (b) CVs of Co-MOF/TM in 0.1 M PBS with varying  $\text{H}_2\text{O}_2$  concentrations at a scan rate of  $50 \text{ mV s}^{-1}$ . (c) CVs obtained at Co-MOF/TM in 0.1 M PBS with 1 mM  $\text{H}_2\text{O}_2$  at different scan rates from 20 to  $200 \text{ mV s}^{-1}$ .

showed that the current density only showed slight decline during multiple cycles in 0.1 M PBS containing 1.0 mM  $\text{H}_2\text{O}_2$ . The relative standard deviation (RSD) of testing on 6 different Co-MOF/TM electrodes is 0.63% and the RSD of 6 parallel measurements is 0.91%, respectively. These results suggested the satisfying stability and repeatability of the Co-MOF/TM as the working electrode.

### 3.3. Analysis of real sample assay

The anti-interference property is a major concern for nonenzymatic biosensors to detection  $\text{H}_2\text{O}_2$ . Thus, the common electroactive species, including uric acid (UA), dopamine (DA), ascorbic acid (AA) and NaCl were chosen to verify the anti-interference performance of Co-MOF/TM. As shown in Fig. 4a, except  $\text{H}_2\text{O}_2$ , none of these interfering substances cause any observable change in the amperometric current for the proposed sensor, which indicated that the Co-MOF/TM has good selectivity towards  $\text{H}_2\text{O}_2$ . Furthermore, the detection of the trace amount of  $\text{H}_2\text{O}_2$  secreted

from living cells was successfully performed with this developed sensor. We chose A549 cells as model cells and Phorbol-12-myristate-13-acetate (PMA) as stimulant to make cells produce  $\text{H}_2\text{O}_2$  [33]. As shown in Fig. 4b, when PMA was added to 20 mL PBS containing  $4 \times 10^7$  A549 cells (pH = 7.4), the amperometric current response was significantly enhanced, while the cells without being treated with PMA or PMA without cells had no signal. This phenomenon demonstrated that the recorded current came from the response with  $\text{H}_2\text{O}_2$ , which released from the A549 cells with the stimulation of PMA.

### 4. Conclusion and perspective

In conclusion, a composite nanosheet array of Co-MOF/TM was developed by in-situ growing Co-MOF on TM to fabricate a non-enzymatic electrochemical sensor for detection of  $\text{H}_2\text{O}_2$  released from living cells. Due to the unique properties of Co-MOF, the proposed sensor showed high sensitivity and selectivity to  $\text{H}_2\text{O}_2$ . Moreover, when the developed sensor was

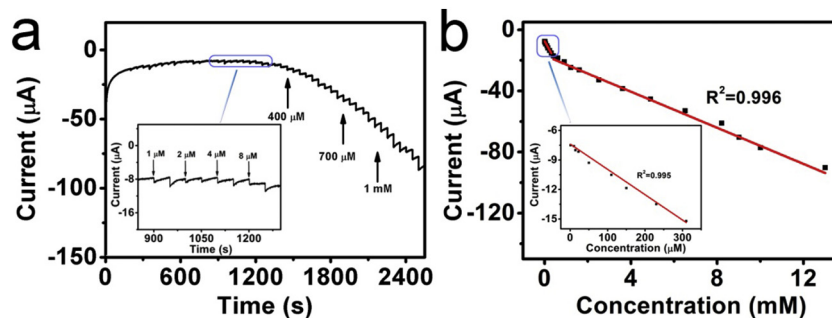


Fig. 3. (a) Amperometric response of Co-MOF/TM to the successive addition of  $\text{H}_2\text{O}_2$  in 0.1 M PBS. The inset shows the amperometric response of  $\text{H}_2\text{O}_2$  at low concentration. (b) Calibration curve of current response vs.  $\text{H}_2\text{O}_2$  concentration.

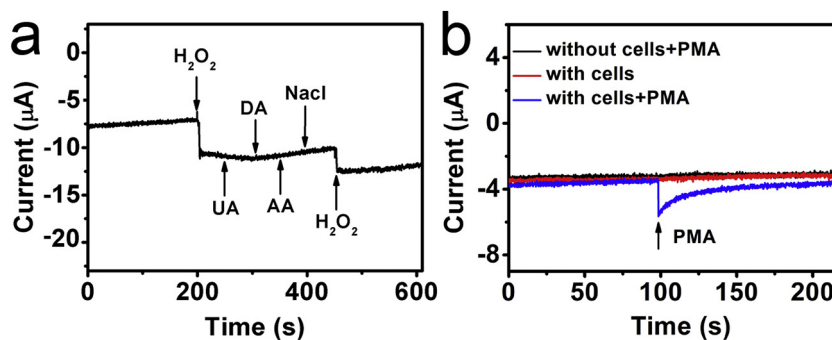


Fig. 4. (a) Amperometric response of Co-MOF/TM under the addition of 1 mM  $\text{H}_2\text{O}_2$  followed by some common interferences in 0.1 M PBS. (b) Amperometric response of Co-MOF/TM to the stimulation in 0.1 M PBS with and without A549 cells.

applied to monitoring  $\text{H}_2\text{O}_2$  released from A495 cells, satisfactory results were achieved. The results of this study showed high perspective for sensing other biomolecules using other active MOFs as electrocatalytic electrodes.

#### Credit author statement

The corresponding author is responsible for ensuring that the descriptions are accurate and agreed by all authors. The role(s) of all authors are listed as below:

**Lian Xia:** Methodology, Software; **Xiaoqian Luan:** Data curation, Writing-Original draft preparation; **Fengli Qu:** Supervision; **Limin Lu:** Writing- Reviewing and Editing.

#### Declaration of Competing Interest

The authors declare that they have no known competing financial interests or personal relationships that could have appeared to influence the work reported in this paper.

#### Acknowledgements

This work was supported by the National Natural Science Foundation of China (21775089, 21671118, 21505084), Outstanding Youth Foundation of Shandong Province (ZR2017JL010), the Key Research and Development Program of Jining City (2018ZDGH032) and Taishan scholar of Shandong Province.

#### Appendix A. Supplementary data

Supplementary data to this article can be found online at <https://doi.org/10.1016/j.jelechem.2020.114553>.

#### References

- [1] S.G. Rhee,  $\text{H}_2\text{O}_2$ , a necessary evil for cell signaling, *Science* 312 (2006) 1882–1883.
- [2] T. Finkel, M. Serrano, M.A. Blasco, The common biology of cancer and ageing, *Nature* 448 (2007) 767–774.
- [3] W.R. Markesbery, Oxidative stress hypothesis in Alzheimer's disease, *Free Radic. Biol. Med.* 23 (1997) 134–147.
- [4] N. Houstis, E.D. Rosen, E.S. Lander, Reactive oxygen species have a causal role in multiple forms of insulin resistance, *Nature* 440 (2006) 944–948.
- [5] M.T. Lin, M.F. Beal, Mitochondrial dysfunction and oxidative stress in neurodegenerative diseases, *Nature* 443 (2006) 787–795.
- [6] W. Wu, J. Li, L. Chen, Z. Ma, W. Zhang, Z. Liu, Y. Cheng, L. Du, M. Li, Bioluminescent probe for hydrogen peroxide imaging in vitro and in vivo, *Anal. Chem.* 86 (19) (2014) 9800–9806.
- [7] Y. Dong, J. Zheng, Environmentally friendly synthesis of co-based zeolitic imidazolate framework and its application as  $\text{H}_2\text{O}_2$  sensor, *Chem. Eng. J.* 392 (2020) 123690.
- [8] X. Jiang, H. Wang, R. Yuan, Y. Chai, A novel functional 3D porous conductive polymer hydrogels for sensitive Electrochemiluminescence in situ detection of  $\text{H}_2\text{O}_2$  released from live cells, *Anal. Chem.* 90 (2018) 8462–8469.
- [9] M.C.Y. Chang, A. Pralle, E.Y. Isacoff, C.J. Chang, A selective, cell-permeable optical probe for hydrogen peroxide in living cells, *J. Am. Chem. Soc.* 126 (2004) 15392–15393.
- [10] M. Tarvina, B. McCordb, K. Mount, K. Sherlachd, M.L. Miller, Optimization of two methods for the analysis of hydrogen peroxide: high performance liquid chromatography with fluorescence detection and high performance liquid chromatography with electrochemical detection in direct current mode, *J. Chromatogr. A* 1217 (2010) 7564–7572.
- [11] E.C. Hurdis, R. Hendrik, Accuracy of determination of hydrogen peroxide by cerate Oxidimetry, *Anal. Chem.* 26 (1954) 320–325.
- [12] D.W. King, W.J. Cooper, S.A. Rusak, B.M. Peake, J.J. Kiddle, D.W. Sullivan, M.L. Melamed, C.R. Morgan, S.M. Theberge, Flow injection analysis of  $\text{H}_2\text{O}_2$  in natural waters using Acridinium Ester Chemiluminescence: method development and optimization using a kinetic model, *Anal. Chem.* 79 (2007) 4169–4176.
- [13] G. Bitner, E.A. Dubikovskaya, C.R. Bertozzi, C.J. Chang, In vivo imaging of hydrogen peroxide production in a murine tumor model with a chemoselective bioluminescent reporter, *PNAS* 107 (2010) 21316–21321.
- [14] A.H. Keihan, R.R. Karimi, S. Sajjadi, Wide dynamic range and ultrasensitive detection of hydrogen peroxide based on beneficial role of gold nanoparticles on the electrochemical properties of prussian blue, *J. Electroanal. Chem.* 862 (2020) 114001.
- [15] H. Beitollahi, S.G. Ivari, M. Torzadeh-Mahani, Application of antibody nanogold ionic liquid carbon paste electrode for sensitive electrochemical immunoassay of thyroid-stimulating hormone, *Biosens. Bioelectron.* 110 (2018) 97–102.

- [16] S. Xu, X. Huang, Y. Chen, Y. Liu, W. Zhao, Z. Sun, Y. Zhu, X. Liu, C.-P. Wong, Silver nanoparticle-enzyme composite films for hydrogen peroxide detection, *ACS Appl. Nano Mater.* 2 (2019) 5910–5921.
- [17] B. Liu, X. Wang, Y. Zhai, Z. Zhang, H. Liu, L. Li, H. Wen, Facile preparation of well conductive 2D MOF for nonenzymatic detection of hydrogen peroxide: relationship between electrocatalysis and metal center, *J. Electroanal. Chem.* 858 (2020) 113804–113812.
- [18] L. Kong, Z. Ren, N. Zheng, S. Du, J. Wu, J. Tang, H. Fu, Interconnected 1D  $\text{Co}_3\text{O}_4$  nanowires on reduced graphene oxide for enzymeless  $\text{H}_2\text{O}_2$  detection, *Nano Res.* 8 (2014) 469–480.
- [19] W. Chen, S. Cai, Q. Ren, W. Wen, Y. Zhao, Recent advances in electrochemical sensing for hydrogen peroxide: a review, *Analyst* 137 (2012) 49–58.
- [20] J. Liu, X. Bo, Z. Zhao, L. Guo, Highly exposed Pt nanoparticles supported on porous graphene for electrochemical detection of hydrogen peroxide in living cells, *Biosens. Bioelectron.* 74 (2015) 71–77.
- [21] X. Zhang, W. Sun, H. Du, R. Kong, F. Qu, A Co-MOF nanosheet array as a high-performance electrocatalyst for the oxygen evolution reaction in alkaline electrolytes, *Inorg. Chem. Front.* 5 (2018) 344–347.
- [22] S. Wang, C.M. McGuirk, J.A. Mason, C.A. Mirkin, Metal-organic framework nanoparticles, *Adv. Mater.* 37 (2018) 1800202.
- [23] N.A.M. Barakat, M.S. Khil, F.A. Sheikh, H.Y. Kim, Synthesis and optical properties of two cobalt oxides ( $\text{CoO}$  and  $\text{Co}_3\text{O}_4$ ) nanofibers produced by electrospinning process, *J. Phys. Chem. C* 112 (2008) 12225–12233.
- [24] Y. Ding, Y. Wang, L.A. Su, M. Bellagamba, H. Zhang, Y. Lei, Electrospun  $\text{Co}_3\text{O}_4$  nanofibers for sensitive and selective glucose detection, *Biosens. Bioelectron.* 26 (2010) 542–548.
- [25] X. Wang, M. Wang, S. Feng, D. He, P. Jian, Controlled synthesis of flower-like cobalt phosphate microsheet arrays supported on Ni foam as a highly efficient 3D integrated anode for non-enzymatic glucose sensing, *Inorg. Chem. Front.* 7 (2020) 108–116.
- [26] F.Y. Xie, X.Q. Cao, F.L. Qu, A.M. Asiri, X.P. Sun, Cobalt nitride nanowire array as an efficient electrochemical sensor for glucose and  $\text{H}_2\text{O}_2$  detection, *Sensor. Actuat. B-chem.* 255 (2018) 1254–1261.
- [27] J. Wang, H. Shen, C. Huang, Q. Ma, Y. Tan, F. Jiang, C. Ma, Q. Yuan, Highly efficient and multidimensional extraction of targets from complex matrices with aptamers-driven recognition, *Nano. Res.* 8 (2017) 145–156.
- [28] B. Wang, X.L. Lv, D. Feng, L.H. Xie, J. Zhang, M. Li, Y. Xie, J.R. Li, H.C. Zhou, Highly stable Zr (IV)-based metal-organic frameworks for the detection and removal of antibiotics and organic explosives in water, *J. Am. Chem. Soc.* 19 (2016) 6204–6216.
- [29] X. Zhang, Sun Weidi, H. Du, R.M. Kong, F. Qu, A Co-MOF nanosheet array as a high-performance electrocatalyst for the oxygen evolution reaction in alkaline electrolytes, *Inorg. Chem. Front.* 5 (2018) 344–347.
- [30] Z. Yao, X. Zhang, F. Peng, H. Yu, H. Wang, J. Yang, Novel highly efficient alumina-supported cobalt nitride catalyst for preferential CO oxidation at high temperatures, *Int. J. Hydrog. Energy* 36 (2011) 1955–1959.
- [31] Y. Zhang, B. Ouyang, J. Xu, G. Jia, S. Chen, R.S. Rawat, H.J. Fan, Rapid synthesis of cobalt nitride nanowires: highly efficient and low-cost catalysts for oxygen evolution, *Angew. Chem. Int. Ed.* 55 (2016) 8670–8674.
- [32] L. Long, H. Liu, X. Liu, L. Chen, S. Wang, C. Liu, S. Dong, J. Jia, Co-embedded N-doped hierarchical carbon arrays with boosting electrocatalytic activity for in situ electrochemical detection of  $\text{H}_2\text{O}_2$ , *Sensor Actuat B-Chem.* 318 (2020) 128242.
- [33] H. Du, X. Zhang, Z. Liu, F. Qu, A supersensitive biosensor based on  $\text{MoS}_2$  nanosheet arrays for the real-time detection of  $\text{H}_2\text{O}_2$  secreted from living cells, *Chem. Commun.* 55 (2019) 9653–9656.